# Collision broadening of the Sr-ion resonance line from the line core to the near-wing region

H. Harima, K. Tachibana, and Y. Urano
*Department of Electronics, Kyoto Institute of Technology, Matsugasaki, Kyoto 606, Japan*
(Received 11 August 1986)

Profiles of the singly ionized strontium resonance line at 421.6 nm ($4p\ ^2P_{1/2}$—$4s\ ^2S_{1/2}$) which are collisionally broadened by argon have been measured from the line core to near-wing region (within the distance of $\Delta\nu \lesssim 50\ \mathrm{cm}^{-1}$ from the line center). The observed broadening rate of the core is $(1.87\pm0.25)\times10^{-20}\ \mathrm{cm}^{-1}/\mathrm{cm}^{-3}$ at 690 K. A clearly asymmetric profile has been observed in the wing region. These results are discussed by considering semiclassical impact and quasistatic theories combined with theoretical interaction potentials for the $Sr^+$-Ar pair which were previously reported by the present authors.

## I. INTRODUCTION

In recent years profiles of atomic and molecular spectral lines which are collisionally broadened by foreign gases have been intensively studied to provide critical tests of sophisticated calculations of collisional interactions.[1] However, previous measurements were mostly done on neutral species and data on ions are obviously insufficient.[2] For example, singly ionized group-II*a* metals have received little attention although their lines often show important features in solar and stellar spectra. In addition to such astrophysical applications, singly ionized II*a* metals are amenable to theoretical treatments of collision problems, since they have isoelectronic structures as neutral alkali metals, i.e., the so-called single-valence-electron system.

From this viewpoint we have studied in a preceding paper[3] theoretical interaction potentials for singly ionized alkaline-earth-metal and rare-gas atom pairs using a pseudopotential model of Baylis,[4] and explained previous line-core data to a reasonable extent by a semiclassical impact approximation. One of the outstanding differences of potentials between neutral colliding pairs and ion—neutral-atom pairs is that in the former case the long-range interaction is dominated by a weak van der Waals interaction, while in the latter case a strong polarization force between a point charge and an induced dipole appears.

We have shown in the preceding paper[3] that this situation causes relatively deep potential wells at short internuclear distance. Thus it is an interesting topic to discuss how these characteristic potential features will affect the collisionally perturbed line profiles.

For the $Sr^+$-Ar pair there is only one previous measurement by Giles and Lewis[2] for the line-core region at 608 K using a flow-lamp technique. We have found in the preceding impact analysis[3] that their value of the broadening rate can be reproduced accurately by our potentials, and that relatively distant collisions with impact parameter $\rho \simeq 14$ a.u. give dominant contributions to the rate. To check the validity of shorter-range potentials rigorously, we must make line-core experiments at higher temperatures or proceed to profile measurement in the wing region. Such ambiguities of impact analyses in assessing potentials of a particular range of internuclear distance commonly occur, because, as is well known, impact approximations are based on an averaging over uncorrelated and completed collisions for various collisional geometries. In contrast, wing data interpreted with quasistatic theories have presented critical tests of potentials at particular internuclear distance, even though the neglect of time dependence of the radiative process often produces unrealistic contours near potential extrema.[1] From this viewpoint, we have extended in this paper the profile measurement to a wing region within the wave-number distance from the line center $\Delta\nu \lesssim 50\ \mathrm{cm}^{-1}$. To the authors' knowledge, this is the first observation of the wing profile of ionic II*a* elements. In addition we have measured the line-core profile to deduce the broadening rate at 690 K. It will be interesting to compare our result with that of Giles and Lewis[2] at 608 K. Since we use a hollow-cathode discharge lamp, there is a possibility[2] that large fringing electric fields may drive ions causing spurious shifts of line core. Therefore in this experiment collisional shift was not measured.

The most important point of this paper that we would like to emphasize from the theoretical viewpoint is that the present observation from the line core to a wing region can be explained to a reasonable extent by a unique theoretical interaction potential.[3] As described above, a characteristic feature of potentials appears in rather short-range interactions with deep potential wells. Although the present wing measurement can not clarify such short-range interactions as done by extreme far-wing experiments of Gallagher and co-workers[5] for alkali-metal—rare-gas pairs, the increase of potential information toward shorter-range internuclear distance than previous line-core experiment is clearly demonstrated.

## II. EXPERIMENTS AND RESULTS

### A. Line-core measurement

The experimental arrangement is shown in Fig. 1. The light source is a hollow-cathode discharge tube which has

 

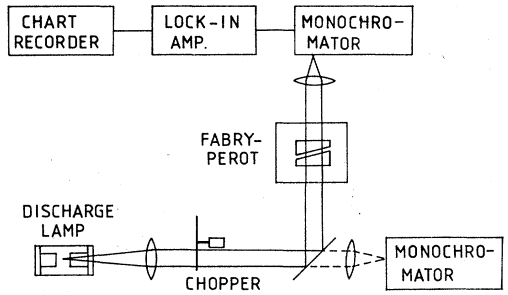


FIG. 1. Experimental arrangement. The dashed line denotes optical path for the wing-region experiment.

a similar construction to that of Kielkopf and Knollenberg.[6] The electrodes were made of stainless-steel tubes of inner and outer diameters 6 and 10 mm, respectively, and were separated by about 10 cm from each other. They were installed in a ceramic tube of 24-mm inner diameter and 30-cm length. The ceramic tube is heated electrically in the central region of about 20-cm length to evaporate a piece of Sr metal placed at the center of the tube. The light emission of $Sr^+$ mainly comes out from the space between the two electrodes. The temperature distributions in the central region of the tube were measured by a thermocouple which was inserted along the tube axis. Another thermocouple for a temperature controller was attached to the outer wall of the ceramic tube. The Ar pressure was varied from a few Torr to 70 Torr. The cell temperature was kept at about 690 K. The temporal fluctuation was less than 1° during one scan of profile. Although we could get somewhat better stability of discharge at higher temperatures, the emission profiles were severely distorted by self-absorption. The discharge current was kept at about 10 mA by a constant current source.

A pressure-scanned Fabry-Perot étalon was used as our spectrometer. Its free spectral range was about 690 mK (mK$=10^3$ cm$^{-1}$). As a predisperser we used an Ebert-type monochromator of 50-cm focal length and spectral dispersion of about 1.7 nm/mm. A plate with a pinhole of 0.5-mm diameter was put just before the entrance slit. The effective finesse of the étalon was about 23 including the pinhole or aperture finesse. The light from the discharge tube was mechanically chopped and the signal from a photomultiplier was detected by a lock-in amplifier.

A typical profile is shown in Fig. 2, where the observed emission intensities are plotted against the wave-number distance from the line center. In analyzing the data to extract collisional-broadening component, we assume that (i) the profiles consist of several hyperfine structure (hfs) components which are convoluted with the instrumental function of the étalon, (ii) these hfs components are described by the same Voigt profile, and (iii) the observed profiles may be somewhat distorted by self-absorption. These factors were treated as follows.

Firstly for hfs, the resonance line at 421.6 nm has seven components.[7,8] To simplify the problem, we have grouped small components at their center-of-gravity frequencies and only four components were considered as shown by bold lines in Fig. 2. The instrumental function was considered as follows. When the étalon plates have a high reflection finesses and small imperfections of flatness and parallelism, it is well approximated by a Voigt profile whose Lorentzian component $\gamma_I^R$ is determined by the reflection finesse $N_e$ or reflectivity $R$, and whose Gaussian component is determined by the above imperfections. From transmission data we estimated $R$ ($\simeq$0.95) and obtained $\gamma_I^R \simeq 12$ mK [full width at half maximum (FWHM) is used in this paper unless specified] using an approximate formula of Ballik.[9] From a nominal value of the plate flatness ($\simeq\lambda/100$) we can make a rough estimate for the Gaussian component; however, the other factor due to parallelism of plates remains uncertain. Therefore we have left the instrumental Gaussian component as an adjustable parameter in fitting the observed profiles by calculated ones.

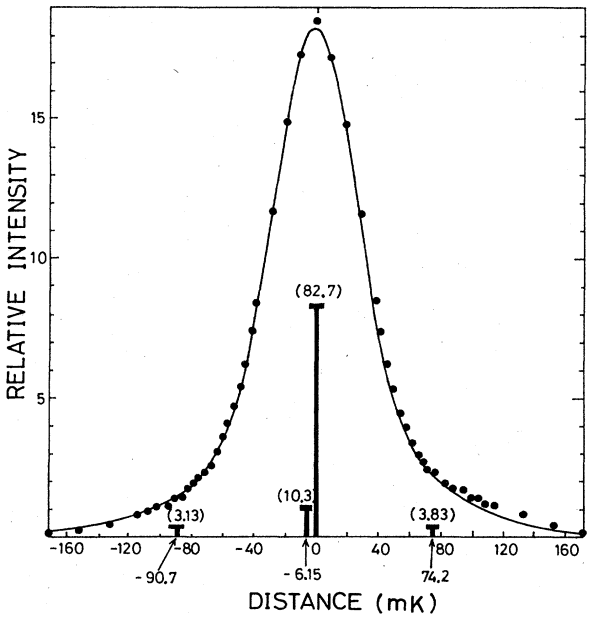


FIG. 2. Typical line-core profile observed at 690 K with Ar 28 Torr (●). The best fit to the profile is shown by the solid curve. Bold vertical lines denote positions of the assumed hfs components, whose weights are shown in the parentheses in percentage. The abscissa shows wave-number distance from the main hfs component in mK ($=10^{-3}$ cm$^{-1}$). Wavelength increases from right to left.

Next we consider the Voigt profile which describes the line shape of hfs. The Gaussian contribution (i.e., Doppler broadening) is calculated as $\gamma_D=48$ mK at 690 K. We assume the Lorentzian component is mainly determined by collisional broadening by Ar, since other contributions such as Stark broadening due to charged particles are negligibly small by the following reason. From the optical depth at line center $\tau_0$ ($\lesssim$0.3) which was measured by Harrison's self-absorption method,[10] we estimated[11] the density of $Sr^+$ in the ground state as $n \lesssim 6\times10^9$ cm$^{-3}$. Then, including populations in excited states, total

$Sr^+$ density would be roughly of the order of $10^{10}$ $cm^{-3}$. In our discharge condition ionization of Ar can be neglected, thus we may assume that the electron density is of the same order of magnitude as that of $Sr^+$. Since Stark broadening coefficient would be[12] of the order of $10^{-15}$ to $10^{-14}$ $mK/cm^{-3}$, the Stark contribution by electrons could be well neglected. Broadening due to collisions with $Sr^+$ itself could be neglected by a similar reasoning.[13] Natural broadening can be calculated[11] from a known transition probability[14] as $\gamma_N = 0.7$ mK.

Finally the distortion due to self-absorption is considered. Baur and Cooper[15] have shown that, when Lorentzian component $\gamma_L$ is large compared with a Gaussian one, a finite optical depth $\tau_0$ ($\lesssim 1$) leads to an additional Lorentzian width $\sim \gamma_L \tau_0/4$ to the observed profile. In our case the Gaussian component (i.e., Doppler width) is large, thus their result can not be used straightforwardly. But by a similar analysis[16] we can estimate that the additional Lorentzian width would be less than 10% in the present experiment, and the resultant error in the collisional-broadening rate would be less than 5%.

An example of the calculated best-fit profile to the observed one is shown in Fig. 2 by the solid curve. In Fig. 3 deduced Lorentzian-broadening components are plotted against the Ar pressure. The slope of a linear fit to the points gives the collisional-broadening rate $\gamma_C/n = (1.87 \pm 0.25) \times 10^{-20}$ $cm^{-1}/cm^{-3}$. The error bar is determined by the scatter of data points and possible error due to self-absorption. The intercept of the line with the ordinate gives Lorentzian components due to other than the collisional broadening, i.e., $\gamma_I^R + \gamma_N$. In fitting for various Ar pressures shown in Fig. 3, the total Gaussian component remained constant at $55.2 \pm 2.7$ mK. Subtracting the Doppler contribution (=48 mK), the remainder might be attributed to the imperfections of étalon plates described above.

### B. Wing-region measurement

Structure of the discharge tube is the same as that used in the line-core experiment except that the electrode distance has been changed. To operate at relatively high pressures of Ar from 100 to 700 Torr with good stability of discharge, the distance between electrodes was decreased to about 20 mm. The emission intensity in the wing region increased with the density of neutral Sr, thus the cell temperature was raised to about 900 K. The discharge current was kept at about 20 mA. Light emission from the discharge tube was mechanically chopped and directly imaged on the entrance slit of about 30 $\mu$m width of the Ebert-type monochromator described previously. The instrumental function of the monochromator was measured with 632.8-nm laser line illuminating a diffusing surface at the entrance slit. It was a Gaussian-like shape with FWHM of about 0.04 nm.

A typical observed profile at low-argon pressure (120 Torr) is shown in Fig. 4. We find that the profile has a somewhat long tail to the red side, and in the central region, which is reduced to $\frac{1}{50}$ in magnitude, we can recognize the effect of self-absorption. With the increase of Ar pressure, the growth of red-wing tail was observed and the asymmetry became more pronounced. This is clearly seen in Fig. 5 where a typical profile at high-Ar pressure (739 Torr) is plotted against the distance from the line center in a logarithmic scale. At $\Delta\nu \gtrsim 4$ $cm^{-1}$ the spectral asymmetry is apparent. Before proceeding to further analysis, we must check profile distortion due to the instrumental

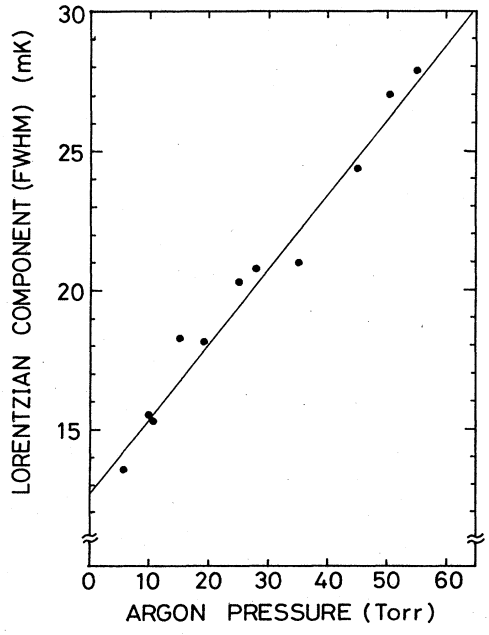


FIG. 3. Deduced Lorentzian-broadening components at 690 K (●). The line shows the best fit to the data points.

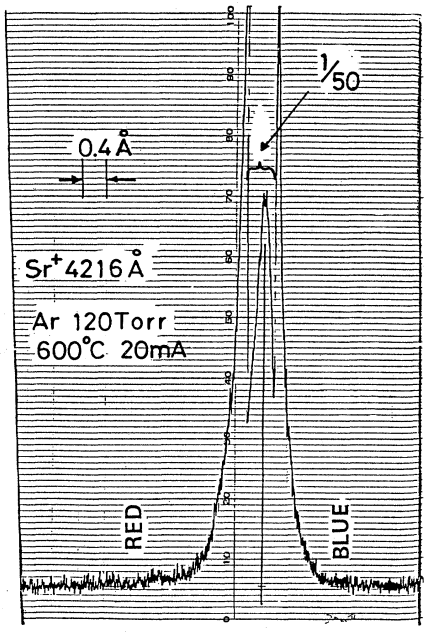


FIG. 4. Typical wing profile observed at relatively low-Ar pressure. Note the central region is reduced to $\frac{1}{50}$ in magnitude.

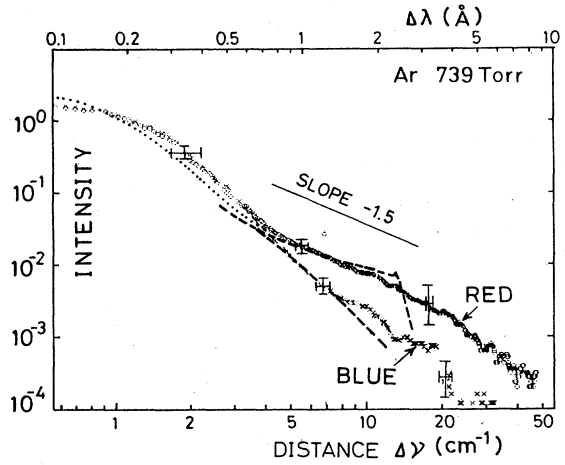


FIG. 5. Typical wing profile observed at relatively high-Ar pressure (shown by the arrows). Dotted curve was obtained by deconvoluting the profile by the instrumental function of the monochromator. Bold dashed curves are UFC calculations. The dependence of $I(\Delta\nu) \propto \Delta\nu^{-1.5}$ is shown for comparison.

function and self-absorption. Since the instrumental function of the monochromator is known, we can estimate the true profile by an appropriate deconvolution treatment of profiles. Estimated true profile is shown by the dotted curve in Fig. 5, where an iterative deconvolution method[17] was used. In this case the instrumental distortion becomes negligible at $\Delta\nu \gtrsim 4$ cm$^{-1}$. Next we consider the self-absorption. Prior to each emission measurement, total absorption[11] $W$ was measured to deduce the optical depth $\tau_0$ at line center. In the example of Fig. 5, we observed $W \simeq 0.002$ nm, then from a curve of growth[11,18] we can obtain $\tau_0 \simeq 2$. In such optically thick lines, the central region must be severely distorted, and numerical reproduction of true profile is very difficult, unless accurate absorption profile is known.[11,19] However, fortunately in our case we can estimate that such distortion appears mainly in the central region of the profile at $\Delta\nu \lesssim 1$ cm$^{-1}$, and the outer-wing region is effectively free of such distortion (see Appendix). Thus this is the region we center our discussion on later. In our experiment $W$ changed slightly with Ar pressure from about 0.001 to 0.002 nm, but the above estimation for the distorted region holds similarly.

## III. DISCUSSION

### A. Potential

The aim of this section is to discuss present results using theoretical interaction potentials of $Sr^+$-Ar pair calculated previously by the present authors.[3] First we briefly review some points on the relevant molecular states $A\,^2\Pi_{1/2}$ and $X\,^2\Sigma_{1/2}$ which tend, respectively, to $5p\,^2P_{1/2}$ and $5s\,^2S_{1/2}$ states of $Sr^+$ at infinite internuclear distance (i.e., the upper and lower states of the 421.6-nm line). They show the same attractive character at large internuclear distance; their collisional perturbation is represented by the polarization force $-\alpha e^2 R^{-4}/2$, where $\alpha$ is the dipole polarizability of Ar, $e$ is the elementary charge, and $R$ is the internuclear distance. However, at smaller internuclear distance ($R \lesssim 20$ a.u.), the upper state $A\,^2\Pi_{1/2}$ shows much more attractive character than the other, and at $R \simeq 6$ a.u. it has a deep well with depth $\sim 1300$ cm$^{-1}$. In Fig. 6(a) the potential shapes are shown for $R > 10$ a.u. As we will see later, this range of internuclear distance is deeply related to the present analysis. If we take the difference of the two molecular potentials, $\Delta V = V(A\,^2\Pi_{1/2}) - V(X\,^2\Sigma_{1/2})$, the above polarization terms cancel. This is graphically shown in Fig. 6(b), where the leading term at large $R$ is proportional to $-R^{-8}$ instead of $-R^{-4}$.

### B. Analysis of broadening rate

Here we consider the observed collision-broadening rate by a semiclassical treatment of impact approximation.[3,20] If perturber density is low and collisions have short durations, the spectral line shape takes a Lorentzian form with the width $\gamma$ (HWHM) and shift $\beta$ given by

$$\gamma + i\beta = 2\pi n \bar{v} \int_0^\infty [1 - \Pi(\rho)] \rho \, d\rho \,, \tag{1}$$

where $n$ is the perturber density, $\bar{v}$ is the average relative

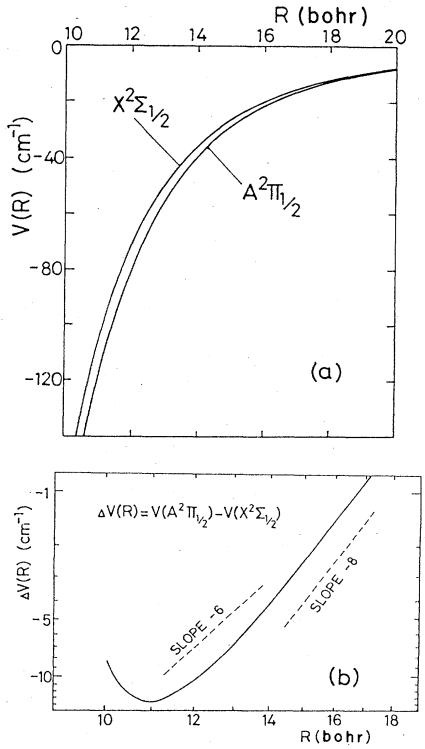


FIG. 6. (a) Theoretical interaction potentials of relevant molecular states for $Sr^+$-Ar pair (Ref. 3) and (b) their difference. The dependences of $\Delta V(R) \propto -R^{-6}$ and $-R^{-8}$ are shown for comparison.

velocity, and $\rho$ is the impact parameter. $\Pi(\rho)$ is given by[21]

$$\Pi(\rho)=\sum_{m_i,m_f,M}\begin{pmatrix} j_f & 1 & j_i \\ m_f & M & -m_i \end{pmatrix}^2 \langle j_i m_i \mid S \mid j_i m_i \rangle \times \langle j_f m_f \mid S^{-1} \mid j_f m_f \rangle , \quad (2)$$

where $|j_f,m_f\rangle$ and $|j_i,m_i\rangle$ denote the ground and excited states of strontium ion, respectively, and $S$ is the scattering matrix. Since the fine-structure splitting of $5P$ states of $Sr^+$ is large (801 $cm^{-1}$), we may assume that there is no nonadiabatic coupling of $A\,^2\Pi_{1/2}$ state with nearby molecular states. Then, using a rotating frame, the $S$ matrix for the excited states takes the form[3,20,22]

$$S=\begin{pmatrix} \exp\left[-i/\hbar\int_{-\infty}^{\infty}(V_\Pi+V_R)dt\right] & 0 \\ 0 & \exp\left[-i/\hbar\int_{-\infty}^{\infty}(V_\Pi-V_R)dt\right] \end{pmatrix}, \quad (3)$$

where $V_\Pi$ denotes the interaction potential of $A\,^2\Pi_{1/2}$ state, and $V_R$ gives the nondiagonal correction term due to the frame rotation. We assume that perturbers follow curved trajectories determined by the classical law of energy conservation

$$\frac{dR}{dt}=\pm\bar{v}\left[1-\frac{\rho^2}{R^2}-\frac{V_\Pi(R)}{E}\right]^{1/2}, \quad (4)$$

where $E$ is the initial kinetic energy. The term $V_\Pi/E$ determines the trajectory deflection from a straight path. In Table I calculated results are compared with experimental results. The theoretical value of broadening rate at 690 K is in agreement with the experimental result at the lower end of the range of experimental uncertainty. The real part of the integrand in (1), $\mathrm{Re}\rho[1-\Pi(\rho)]$, is plotted in Fig. 7. We can see that collisions with relatively large impact parameters $\rho \gtrsim 12$ a.u. give dominant contribution ($\simeq$70%) to the rate. For such impact parameters trajectory deflection is small, since the contribution of the term $V_\Pi/E$ in (4) is quite small. Therefore we may conclude that the broadening rate is rather sensitive to relatively long-range interactions at $12 \lesssim R \lesssim 15$ a.u., where the difference potential is predominated by $-R^{-8}$ or $-R^{-6}$ term [see Fig. 6(b)].

If we compare our result with that of Giles and Lewis[2] at 608 K (Table I), the broadening rate observed in this experiment is larger than their value by a factor of $1.3\pm0.3$. Although within the experimental uncertainty this factor agrees with our theoretical prediction ($1.60/1.51=1.06$), it seems slightly too large if we consider the small-temperature difference between 608 and 690 K. At present we cannot make a good explanation for this discrepancy. One possibility from our experimental side is that the cell temperature in the discharge region may have been somewhat underestimated. We could not directly measure the temperature by inserting a thermocouple into the region when the discharge was on, since it would greatly perturb the discharge condition. Thus we have estimated it from a temperature-distribution measurement made prior to the discharge experiment. Actually, when the discharge was on, the observed region might be somewhat ($\lesssim$50 K) heated by electron collisions. As for the experiments by Giles and Lewis,[2] there is no definite description of temperature uncertainty. However, if we refer to the experiment on $Ca^+$-Ar pair by Bowman and Lewis[23] who used the same equipment as that of Giles and Lewis[2] it would be within $\sim\pm80$ K.

It is worth noting here that close values to the above prediction can be obtained from a simple classical consideration; when the difference potential is written by an attractive inverse-power potential, $\Delta V(R)=-C_pR^{-p}$, the collision-broadening rate should have a velocity and temperature dependence as[1]

$$\gamma_C/n \propto \bar{v}^{(p-3)/(p-1)} \propto T^{(p-3)/(2p-2)} . \quad (5)$$

As written above, the difference potential for the present colliding pair has $-R^{-8}$ or $-R^{-6}$ dependence in the im-

TABLE I. Broadening and shift rates for the $Sr^+$ 421.6 nm perturbed by Ar ($10^{-20}$ $cm^{-1}/cm^{-3}$). $\gamma_C$ is given in FWHM.

| Calculation | | Experiment | | |
|---|---|---|---|---|
| $\gamma_C/n$ | $\beta/n$ | $\gamma_C/n$ | $\beta/n$ | $T$ (K) |
| 1.60 | −0.44 | 1.87±0.25[a] | | 690 |
| 1.51 | −0.35 | 1.44±0.12[b] | −0.20±0.05[b] | 608 |

[a]Present experiment.
[b]Reference 2.

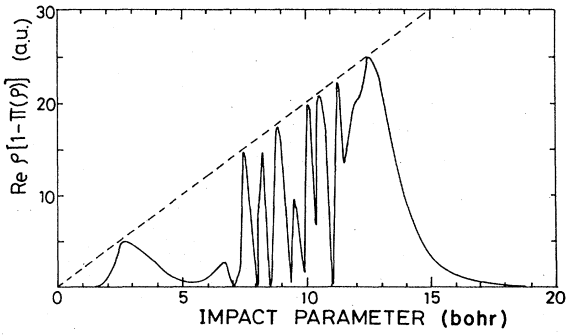


FIG. 7. Real part of $\rho[1-\Pi(\rho)]$ (at 690 K).

portant range of internuclear distance, thus putting $p=6$ and 8 in (5) we may predict a ratio of broadening rates of 690 K to that of 608 K as 1.04—1.05. These values are close to our prediction ($=1.06$).

### C. Analysis of wing profile

As discussed in Sec. II B the central region at $\Delta\nu<1$ $cm^{-1}$ is probably severely self-absorbed, therefore we cannot discuss the line intensity in the normalized unit $I(\nu)/n\int I(\nu)d\nu$. Instead, here we discuss only the relative intensity at $\Delta\nu\gtrsim 3$ $cm^{-1}$, where the profiles are expected to be effectively free of distortions by self-absorption and instrumental function. If we look at the typical profile in Fig. 5, we first notice that the red wing at $4\lesssim\Delta\nu\lesssim 15$ $cm^{-1}$ has $\Delta\nu^{-n}$ dependence with $1.4\lesssim n\lesssim 1.5$. If we recall a well-known result of quasistatic theory[1] that the red wing has $I(\Delta\nu)\propto\Delta\nu^{-(p+3)/p}$ dependence for an inverse-power attractive potential $\Delta V(R)=-C_pR^{-p}$, the present feature indicates that the difference potential for the $Sr^+$-Ar pair has a similar dependence with $6\lesssim p\lesssim 8$. To discuss this point more explicitly, we will calculate a theoretical wing profile by the unified Franck-Condon (UFC) theory of Szudy and Baylis[24] using the calculated potential[3] shown in Fig. 6. Since the observed profile is given in relative intensity, the UFC profile was shifted arbitrarily to the vertical direction until the optimum agreement was obtained. The result is compared in Fig. 5 with the observed profile. The UFC calculation seems to well reproduce some characteristics of the observed profile, e.g., the intensity of blue wing falls more rapidly than red wing as $\Delta\nu$ increases at $\Delta\nu\gtrsim 4$ $cm^{-1}$. However, there are some serious discrepancies; e.g., the UFC red wing has a satellite feature at $\Delta\nu\simeq 13$ $cm^{-1}$ corresponding to a minimum of $\Delta V(R)$ at $R\simeq 11$ a.u. [see Fig. 6(b)], but the observed profile does not show such a drastic change. Red-wing profiles observed at different Ar pressures showed similar characteristics. In addition, at large $\Delta\nu$ the UFC blue-wing intensity seems to fall somewhat more rapidly as $\Delta\nu$ increases than the observation. This sharp decrease was derived as follows. For an inverse-power attractive potential the UFC theory predicts a sharply decreasing (antistatic) blue-wing profile; e.g., for $\Delta V(R)=-C_6R^{-6}$ and $-C_8R^{-8}$, the blue wing is written, respectively, as $\Delta\nu^{-3/2}\exp(-K\Delta\nu^{5/9})$ and $\Delta\nu^{-11/8}\exp(-K'\Delta\nu^{7/2})$, where $K$ and $K'$ ($>0$) are constants determined by $C_6$, $C_8$, and average collision velocity. As is seen in Fig. 6(b), the calculated potential at $R>11$ a.u. is asymptotically described by these potentials. Thus it is quite reasonable that exact calculation of the blue-wing intensity gives a sharp decrease similar to the above dependences.

Anyway the above discrepancies of profiles indicate direction to future improvement of potentials. For example, the discrepancy in the red wing may be improved if the difference potential $\Delta V(R)$ is somewhat more attractive than the present one at small $R$. If so, real Condon points[24] exist and UFC (static) red wing has large intensity at large $\Delta\nu$. From the viewpoint of Baylis' model calculation,[3] the potentials in the relevant $R$ region [Fig. 6(a)] are mainly determined by long-range attractive force due to electrostatic interaction. Then the potential shape is strongly dependent on the selection of valence-electron's wave function, and weakly dependent on other adjustable parameters such as $r_0$ (the rare-gas radius).[24] Thus any better agreement of profiles might be obtained by careful selection of these parameters.

## IV. CONCLUSIONS

We have measured the profile of strontium-ion resonance line collisionally perturbed by argon from the line center to near-wing region. Observed broadening rate of line core shows reasonable agreement with a semiclassical calculation combined with a theoretical interaction potential previously reported. Clearly an asymmetric profile was observed in the wing region. The strong red-wing tail can be explained to some extent by a quasistatic theory, yet there is still some serious discrepancy at large distance from the line center. Better agreement would probably be obtained if we improve short-range potentials at $R<11$ a.u. To discuss this point further, more precise experiment in the far-wing region is expected.

## ACKNOWLEDGMENTS

The authors are very grateful to Mr. T. Ihara, Mr. S. Izeki, Mr. T. Mizushima, Mr. A. Fujimura, Mr. M. Narazaki, and Mr. S. Oshima for the experimental assistance. This work was supported in part by a Grant-in-Aid from the Ministry of Education, Science and Culture of Japan.

## APPENDIX

Here we estimate the spectral region which is severely distorted by self-absorption.[15,16,19] The effect of a finite optical depth $\tau(\Delta\nu)$ in a homogeneous gas is to modify a true emission profile $\phi(\Delta\nu)$ to an emergent one $\Phi(\Delta\nu)$, i.e.,

$$\Phi(\Delta\nu)=\frac{1-\exp[-\tau(\Delta\nu)]}{\tau(\Delta\nu)}\phi(\Delta\nu)\ , \tag{A1}$$

where $\tau(\Delta\nu)$ is the optical depth at a distance $\Delta\nu$ from the line center. We assume $\tau(\Delta\nu)$ is related to $\tau_0$, the optical depth at line center, and the true line profile $\phi(\Delta\nu)$ as

$$\tau(\Delta\nu)=\tau_0[\phi(\Delta\nu)/\phi_0]\ , \tag{A2}$$

where $\phi_0$ is the maximum value of $\phi(\Delta\nu)$ at line center. Suppose $\phi(\Delta\nu)$ is described by a Voigt function whose Gaussian and Lorentzian components are, respectively, given by 53 and 200 mK, and put $\tau_0=2$. This condition corresponds to the case when the distortion is most severe (Ar 700 Torr, 690 K). As $\Delta\nu$ increases the factor in (A1),

$$\{1-\exp[-\tau(\Delta\nu)]\}/\tau(\Delta\nu)\ ,$$

which describes the distortion, rapidly approaches unity. For example, at $\Delta\nu=1$ $cm^{-1}$, which is about five times greater than the line-core width, we get[25] $\phi(\Delta\nu)/\phi_0\simeq 0.01$ and from (A2) $\tau(\Delta\nu)\simeq 0.02$. So that the above distortion

factor is very close to unity,

$$\frac{1-\exp[-\tau(\Delta\nu)]}{\tau(\Delta\nu)} \simeq 1-\frac{\tau(\Delta\nu)}{2} \simeq 0.99 , \quad \text{(A3)}$$

i.e., the spectral distortion is on the order of 1%. Strictly for such large values of $\Delta\nu$ the profile may deviate from a Voigt profile, but it would not significantly influence the above estimation.


[1]N. Allard and J. Kielkopf, Rev. Mod. Phys. **54**, 1103 (1982).

[2]R. G. Giles and E. L. Lewis, J. Phys. B **15**, 2871 (1982).

[3]H. Harima, T. Ihara, Y. Urano, and K. Tachibana, Phys. Rev. A **34**, 2911 (1986).

[4]W. E. Baylis, J. Chem. Phys. **51**, 2665 (1969).

[5]A. Gallagher, *Atomic Physics* (Plenum, New York, 1975), Vol. 4, p. 559.

[6]J. F. Kielkopf and R. B. Knollenberg, Phys. Rev. A **12**, 559 (1975).

[7]M. Heydon and H. Kopferman, Z. Phys. **108**, 232 (1938).

[8]K. Heilig, Z. Phys. **161**, 252 (1961).

[9]E. A. Ballik, Appl. Opt. **5**, 170 (1966).

[10]J. A. Harrison, Proc. Phys. Soc. London **73**, 841 (1959).

[11]A. C. G. Mitchell and M. W. Zemansky, *Resonance Radiation and Excited Atoms* (Cambridge University, London, 1934).

[12]J. Puric, M. Platisa, and N. Konjevic, Z. Phys. **247**, 216 (1971).

[13]H. R. Griem, *Spectral Line Broadening by Plasmas* (Academic, New York, 1974).

[14]W. L. Wiese and G. A. Martin, *Wavelength and Transition Probabilities for Atoms and Atomic Ions,* Natl. Stand. Ref. Data Syst., Natl. Bur. Stand. (U.S.) Circ. No. 68 (U.S. GPO, Washington, D.C., 1980), Pt. II.

[15]J. F. Baur and J. Cooper, J. Quant. Spectrosc. Radiat. Transfer **17**, 311 (1977).

[16]Y. Urano, M. Monju, H. Harima, and K. Tachibana, Jpn. J. Appl. Phys. **20**, 1021 (1981).

[17]P. A. Jansson, *Deconvolution with Applications in Spectroscopy* (Academic, London, 1984).

[18]Here we assume that the line core is described by a Voigt profile composed of Doppler broadening $\gamma_D = 53$ mK and collision broadening by Ar, $\gamma_C = 200$ mK. The value of $\gamma_D$ corresponds to the experimental temperature of 960 K, and $\gamma_C$ was estimated from the present line-core experiment.

[19]A. Corney, *Atomic and Laser Spectroscopy* (Clarendon, Oxford, 1977).

[20]A. Giusti-Suzor and E. Roueff, J. Phys. B **8**, 2708 (1975).

[21]E. L. Lewis, Phys. Rep. **58**, 1 (1980).

[22]E. Roueff and H. Abgrall, J. Phys. (Paris) **38**, 1485 (1977).

[23]N. J. Bowman and E. L. Lewis, J. Phys. B **11**, 1703 (1978).

[24]J. Szudy and W. E. Baylis, J. Quant. Spectrosc. Radiat. Transfer **15**, 641 (1975).

[25]J. T. Davies and J. M Vaughan, Astrophys. J. **137**, 1302 (1963).